Ion behavior in low-power magnetically shielded and unshielded Hall thrusters

L Grimaud, S Mazouffre

Ion behavior in low-power magnetically shielded and unshielded Hall thrusters

L. Grimaud[1], S. Mazouffre[1]

[1] Electric propulsion team, ICARE, CNRS, Orléans (45100), France

E-mail: lou.grimaud@cnrs-orleans.fr

Abstract.

Magnetically shielded Hall thrusters achieve longer lifespan than traditional Hall thruster by reducing wall erosion. The lower erosion rate is attributed to a reduction of the high energy ion population impacting the walls. To investigate this phenomenon the ion velocity distribution functions are measured at several points of interest in the magnetically shielded 200 W ISCT200-MS and the unshielded ISCT200-US. Laser induced fluorescence is used as a non-invasive probing system to spatially resolve the ion behavior. To characterize the discharge, profiles at the center of the discharge channel are taken. Erosion phenomena are investigated by taking measurements of the ion velocity distribution near the inner and outer wall. Some erosion is observed on the magnetic poles of the shielded thruster and laser induced fluorescence measurements are performed there too.

The resulting distribution functions shows a displacement of the acceleration region from inside the channel in the unshielded thruster to downstream of the exit plane in the ISCT200-MS. Near the walls, the unshielded thruster displays both a higher relative ion density as well as a significant fraction of the ions with velocities toward the walls compared to the shielded thruster. Higher proportions of high velocity ions are also observed. Those results are in accordance with the reduced erosion observed. Both shielded and unshielded thrusters have large populations of low velocity ions impacting the magnetic poles. No measurable population of high energy ion is seen.

Submitted to: *Plasma Sources Sci. Technol.*

1. Introduction

Kilowatts class, traditional Hall thrusters (HT) have lifespan of around 10,000 hours [1] which limits their range of application. Small ($\leq$ 300 W) thrusters have even worst performances in that regard, with lifespan limited to a few thousand hours [2]. The limitation comes from the erosion of the discharge channel walls by energetic ions. Applications such as interplanetary and small satellite propulsion require longer lifespan and higher total impulse than what is currently available from Hall thrusters. As such, erosion reduction strategies has been one of the main focus in Hall thruster development in the last few years.

1.1. Magnetic shielding

The magnetic shielding (MS) concept, originating from JPL, is a magnetic topology that has been shown to greatly reduce wall erosion while conserving similar performances to unshielded (US) thrusters[3, 4, 5, 6, 7]. The idea is to reduce the ion velocity and density at the wall. This is achieved by a unique magnetic topologies that features a so called grazing line and by displacing the maximum magnetic field along the center of the discharge channel outside the thruster. The grazing lines are magnetic lines parallel to the thruster walls, originating from the top of the magnetic poles and reaching all the way to the anode area. The high electron mobility along magnetic lines ensures that the electron temperature on those lines is low, as it is the case near the anode. This nearly uniform low electron temperature layer reduces the potential drop experience by the ions in the plasma sheath near the walls. The concave field lines also help directing the ions away from the wall.

Measurements and simulations nearly always show an electric field located at the maximum of the magnetic field[4]. Thus, the external maximum for the magnetic field should push the acceleration region outside the thruster. This means that no high velocity ion should exist inside the discharge channel. Simulations points toward such a behavior but the only experimental measurements of the plasma potential in MS-HT have been done with electrostatic probes. Those kind of probe measurements are known to greatly disturb the discharge when used in such area [8, 9]. Moreover there is significant uncertainties associated with the values obtained with probes in those high gradient, high magnetic field and highly anisotropic conditions.

Erosion inside a MS thruster is reduced by several orders of magnitude and is expected to greatly increase the lifespan of Hall thrusters. However during testing erosion marks appear above the magnetic poles. This erosion could compromise the goal of a long lifespan HT and has been the subject of recent investigations.

The goal of this work is to characterize the ion velocity distribution in three area of interest: in the center of the discharge channel, near the walls in the area corresponding to the high erosion zone in US-HT and above the magnetic poles.

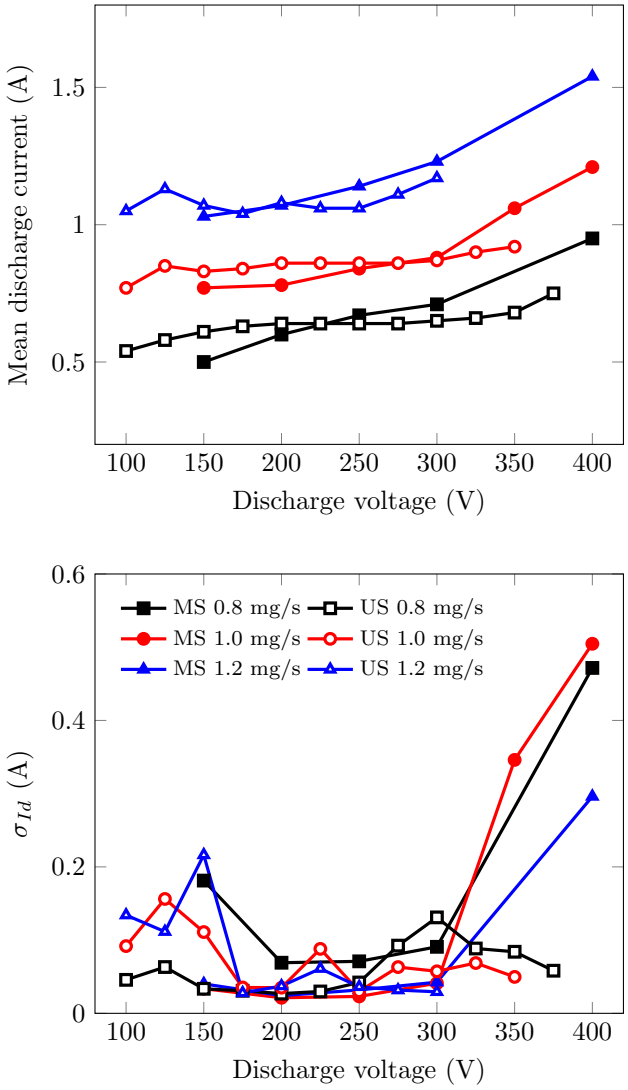

Figure 1. Comparison of the mean and standard deviation of the discharge current between the MS and US 200 W thrusters

1.2. The ISCT200-MS Hall thruster

In this study two Hall thrusters, one magnetically shielded, one unshielded, were used. The ISCT200-MS is the latest iteration in the ISCT (ICARE's Small Customizable Thruster) family. It is a 200 W permanent magnets thruster with a BN-SiO_2 discharge channel. This thruster was built as the magnetically shielded version of the ISCT200-US and shares the same channel geometry, maximum magnetic field and magnetic field gradients along the center of the discharge channel.

1.2.1. Discharge characteristics The ISCT200-US and ISCT200-MS were designed as 200 W thrusters. The ISCT200-MS was tested from 75 W to 600 W. The behavior from 200 to 300 V discharge voltage is really close to the ISCT200-US. As seen on figure 1 the mean discharge current is comparable between the two.

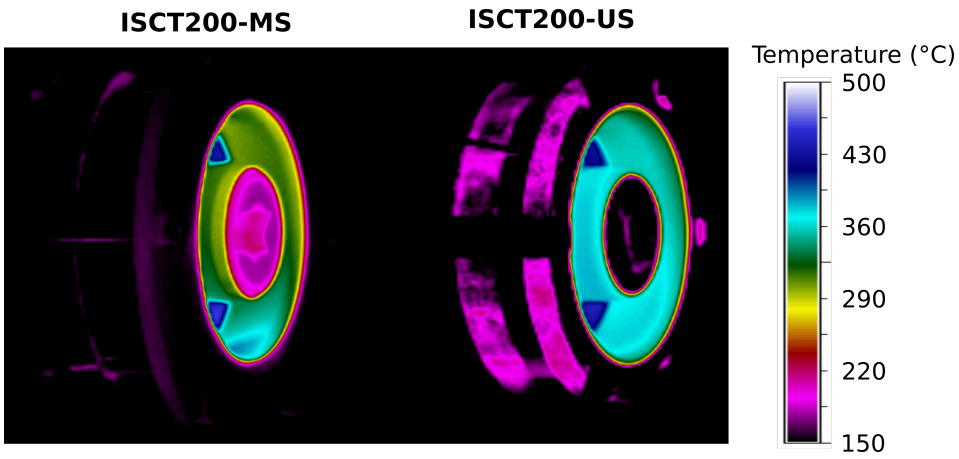

Figure 2. Comparison of the temperature measured by IR imaging at 200 V 1 mg/s.

Figure 1 also shows that the discharge current tends to be less stable in the shielded case for low xenon mass flow rate ($\sim$ 0.8 mg/s) or high discharge voltage (>300 V). Discharge mode transition similar to Conversano's "jet" and "diffuse" modes have also been observed on some occasions [2]. We were able to stabilize the thruster in the less oscillating "diffuse mode" for all the test cases up to a discharge voltage of 300 V. At higher discharge voltage the "jet mode" was the only stable one. While these two modes are not the object of this paper, it is worth mentioning that contrary to Conversano the "jet mode" was observed at high discharge power when it can be assumed that the temperature is the highest. No obvious correlation between mode/plume shape and temperature was observed during thermal studies.

The plume divergence as well as current and propellant utilization efficiency were also measured and are available in the literature [10]. Only small discrepancies have been observed in the divergence and current fraction on the plume between the two thrusters. Propellant utilization was lower in the MS-HT.

1.3. Thermal behavior

The thermal behavior of the thrusters was investigated in a power band ranging from 110 to 220 W. To measure the temperature we used an Optris PI400 IR camera, observing from 7.5 to 13 microns with a resolution of 382x288 pixels, through a ZnSe viewing port. Figure 2 shows a comparison of the two thrusters general thermal behavior at the nominal 200 V 1 mg/s point. Those images are not corrected for emissivity.

The issue with infrared imagery is that the computed temperature is highly dependent on the material emissivity. Through previous infrared studies of Hall thrusters [11] we have a good estimate of the emissivity of the BN-SiO_2 ceramic which allowed us to correct for it in figure 3. Metal surfaces such as the anode can have very different emissivity depending on the surface finish, oxidation level and view angle. Absolute values of the anode temperature are thus not very precise but provide a good idea of the relative temperature difference between the two thrusters.

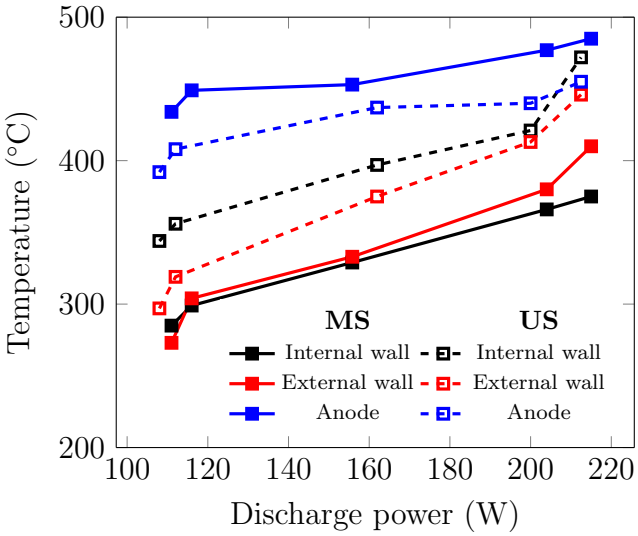

Figure 3. Temperature versus discharge power for the ISCT200-MS and ISCT200-US as measured by IR camera.

The wall temperature is measurably lower in the MS-HT with an internal wall temperature around 60°C colder and external wall temperature 30°C colder on average. These surface measurements seem to show that there is less heat flux at the wall on the MS thruster.

Anode temperature of the MS-HT is higher than for the US-HT (by about 40°C on average). Those results are in accordance with measurements on the H6 where lower temperature were seen on the walls near the exit of the discharge channel while the anode was hotter in the magnetically shielded thruster [12]. This could be explained by the presence of the grazing field lines collecting electrons near the walls and funneling them toward the anode.

2. Experimental setup

2.1. Test facility

Both thrusters were fired in the NExET (New Experiment in Electric Propulsion) vacuum chamber. The vacuum vessel is a 1.8 m × ⌀0.8 m stainless steel cylinder. It is fitted with a large dry pump, a 350 l/s turbomolecular pump and cryogenic pump cooled down to 35 K. The resulting operating pressure is 5×10^{-5} mBar-Xe with a 1.2 mg/s total xenon mass flow rate. This background pressure ensures a momentum exchange mean free path for heavy particles in the order of the chamber length.

2.2. Laser induced fluorescence spectroscopy setup

2.2.1. Overview Laser induced fluorescence (LIF) spectroscopy is an optical diagnostic providing access to the neutral and ion velocity distribution functions (NVDF and IVDF

respectively). The technique itself as well as the setup used at ICARE is presented in more details in [13, 14]. A brief overview is presented here as well as some important details, limitations and side effects relevant to this study.

A narrow-band tunable diode laser is used to excite the $5d^4F_{7/2} \rightarrow 6p^2D^0_{5/2}$ transition of metastable Xe^+ ions. The fluorescence light is collected through a fiber and sent to a photomultiplier via a monochromator to isolate the 541.9 nm fluorescence line. The laser wavelength and fluorescence signal strength allow us to obtain the velocity (by computing the Doppler shift) and relative ion density.

We chose to probe the neutral population starting from the $6s[1/2]^0_2(1s5)$ resonant state, exciting in the near infra-red at 834.91 nm and observing the fluorescence at 473.4 nm. The 823.16 nm resonant transition can also be used, however since the resonant state emits back at 823.16 nm it can be hard to distinguish between signal and reflected or stray light when probing close to a surface.

2.2.2. Setup The setup for the air side is as follow. A single mode tunable laser diode with an external amplifier is used to create the infrared laser beam. A fraction of the main beam is split off Fabry-Pero interferometer to check for mode hops. The wavelength is also measured by a HighFinesse wave-meter with a worst case precision of 70 MHz (corresponding to 60 m/s). Power output of the laser is monitored by a photo-diode. The main beam is modulated by a mechanical chopper and then injected into a 5 µm diameter mono-mode optical fiber. This fiber is used to feed the laser inside the vacuum chamber.

The fluorescence signal is collected by a lens that focuses it into a 200 µm diameter multi-mode optical fiber. Two different lenses were used in this research, for the measurements the walls and at the center of the discharge channel we used a lens 25 mm diameter with a 40 mm focal. Near the magnetic poles, since the fluorescence signal was a lot fainter a 50.8 mm diameter and 38.1 mm focal length one was used.

The collected signal is then fed into a monochromator tuned to the fluorescence wavelength and finally a photo-multiplier. The background noise from spontaneous fluorescence is removed with a lock-in amplifier extracting the signal modulated at the chopper frequency.

This measurement technique is considered non-disturbing to the thruster discharge as the power density of the laser ($\sim 15\ mW/mm^2$) is at least an order of magnitude lower than the power density of the plasma.

Five different areas were studied during this project: the center of the discharge channel (figure 4), the bevels just upstream the exit plane both on the inside and outside wall (figure 9), and both the inner and outer magnetic poles (figure 14).

2.2.3. Limitations and sources of error The positions of the points probed during this study can induce sources of error usually neglected when doing simple axial LIF spectroscopy along the center of the discharge channel.

When measuring velocities normal to the thruster surfaces, the measurement volume is directly in the path of possible laser reflection. Specular reflection would produce a "ghost" mirror image of the VDF centered on v=0 m/s line. This effect is discussed in section 5.2. The exact effects of diffuse reflection are less obvious. It should however manifest itself as general broadening of the obtained VDF.

Some of the areas of interest (magnetic poles and channel walls) are regions of high magnetic fields intensity where the Zeeman effect can become significant. Exact estimation of this effect is complex due to the numerous isotopes of Xenon and the uncertainties in the exact magnetic field topology. During his IVDF measurements over the magnetic pole of the H6 thruster, Jorns estimated that Zeeman effect would result in a 15% overestimation of the ion temperature [15]. Since this paper presents a mostly qualitative, rather than quantitative analysis of the IVDFs, we have not attempted to correct for the Zeeman effect.

2.2.4. Computing the electric field from IVDF From the IVDFs at different positions it is possible to compute the electric field experience by those ions. Different techniques exists which offer different levels of accuracy [16]. We chose to compute the potential drop (V) experienced by the ions by looking at their kinetic energy corresponding to their most probable velocity (v_{mp}) as explained in equation 1.

$$V = \frac{m_{Xe} \cdot v_{mp}^2}{2e} \tag{1}$$

The electric field was then computed with a second order centered difference scheme. Since only the most probable velocity (ie the position of the maximum of the IVDF) is required, this method is fast and is less sensitive to noisy data.

3. Ion behavior at the center of the discharge channel

The ion velocity distributions were first measured at different positions along the center of the discharge channel. Figure 4 shows the location of the probes points as well as the orientation of the laser.

3.1. Ion velocity distribution shape

Ion velocity distributions as well as ion mean and most probable velocities at the center of the discharge channel of classical unshielded thrusters have been extensively described in the literature [17, 18]. A slow moving (few hundreds meter per seconds), thermalized ion group created several millimeters upstream of the exit plane is seen diffusing though the thruster. As it approaches the area of maximum magnetic field the Maxwell distribution changes shape when part of the ions are accelerated and some more are created by the high energy electrons. After the high electric field region the majority of the ions is part of a main thermalized group which has a mean energy corresponding to the discharge

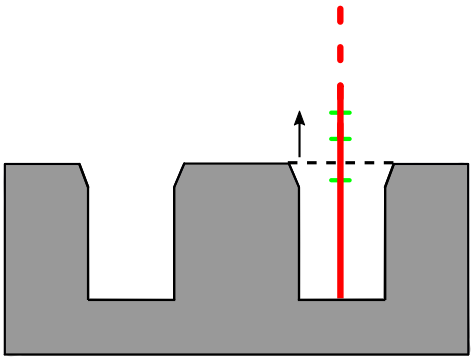

Figure 4. Laser orientation during measures along the center of the discharge channel. The arrow is oriented along the positive velocity direction. The reference position is the exit plane of the thruster

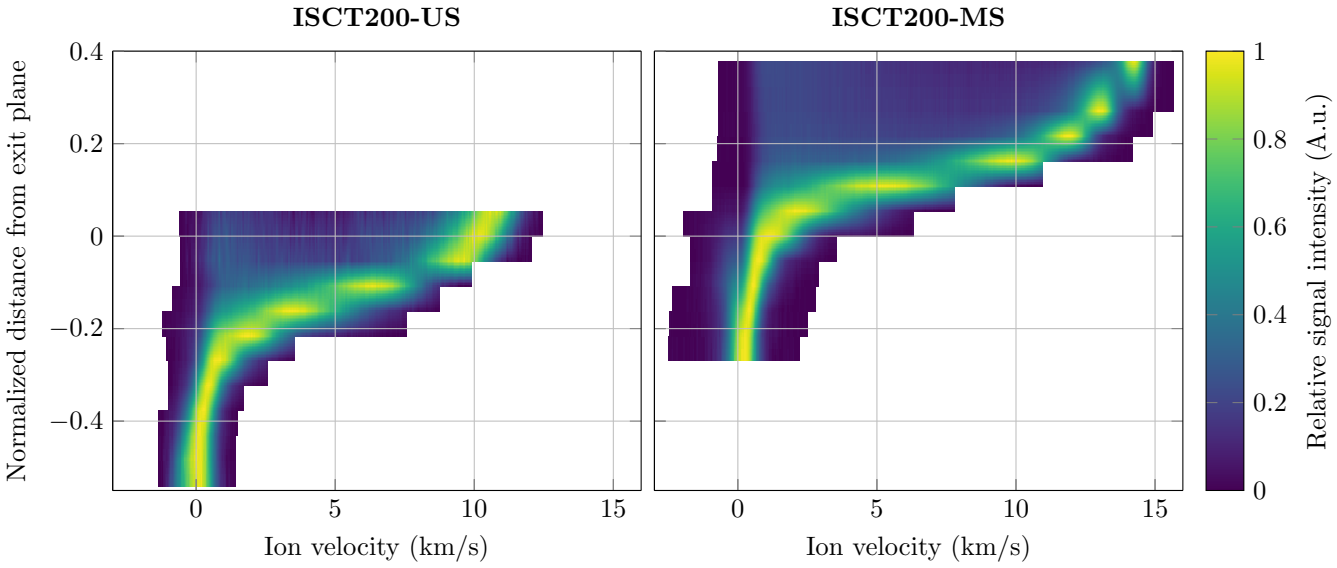

Figure 5. Normalized axial IVDFs along the center of the discharge channel

potential drop. A trail of slower ion is also visible. The origin of those slower ions is not entirely clear but is suspected to be the result of ion/neutral collisions [19].

As illustrated in figure 5, the same three phases are observed for both US and MS thrusters. The positions are simply shifted downstream for the ISCT200-MS.

3.2. Axial electric field

The resulting plasma potential profiles and electric fields are plotted in figure 6. In the case of the magnetically shielded thruster the acceleration region is pushed outside the discharge channel. The maximum value of the electric field is higher but the final most probable velocity of the ions is very similar in the far plume of both thrusters (not displayed in figure 5). We measured 14.5 km/s for the US-HT and 14.7 km/s for the MS-HT. The acceleration region is narrower in the ISCT200-MS.

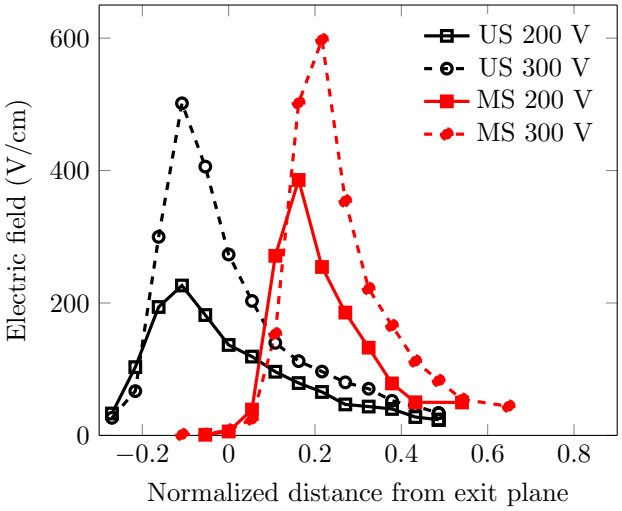

Figure 6. Electric field along the center of the discharge channel

As with US-HT the position of the maximum of the electric field in the MS-HT is located at the maximum of the magnetic field.

3.3. Ion density

It is possible to extract the relative ion density from the IVDF. If the laser wavelength is swept over a large enough range, the integral of the IVDF should capture all the velocity groups and be proportional to the density of the metastable ions. Assuming that the proportion of metastable ions to ground state ions is constant this integral can be considered proportional to the ion density. Absolute values of the ion density would require very careful calibration against a known source and was not done in this work. It is however possible to get the relative density at different points for a given test run.

Figure 7 compares the normalized density profiles in both thrusters. While the absolute density is not known it is not unreasonable to assume that the maximum ion density measured in the MS-HT is either equivalent or even lower (due to being outside the confines of the channel) than in the US-HT. This assumption is supported by how close the discharge characteristics are for those settings. With this assumption the ion density in the discharge channel of the shielded thruster is at least an order of magnitude lower than in a classical one.

3.4. Consequences on erosion

The downstream shift in the position of the ionization and acceleration contributes to the low observed erosion of the magnetically shielded thrusters. While a lot of attention has been dedicated to the behavior of the ions near the walls and to the influence of the "grazing line", the bulk behavior should not be ignored. Not only the ion density is lower in the MS-HT but their bulk axial velocity at the exit plane is also considerably

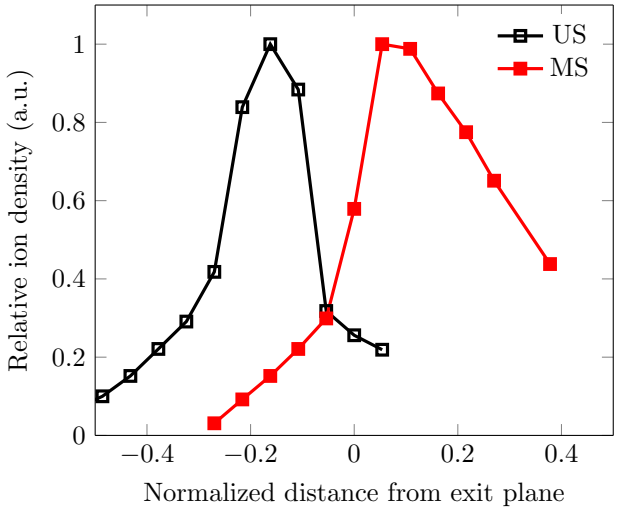

Figure 7. Comparison of relative ion density profiles in US and MS Hall thrusters along the center of the discharge channel at 200 V discharge voltage. The profiles are normalized by their respective maximum value.

lower as they are mostly accelerated outside of the discharge channel. This reduces both the flux and mean energy of the ions inside the thruster.

4. Ion behavior near the walls

4.1. Visual evidences of magnetic shielding

Direct measurements of the erosion rates require expensive and lengthy endurance testing and profilometry measurements which were not available to us. However several visual clues can provide good evidences of the low erosion behavior of the ISCT200-MS.

The most obvious evidence is presented in figure 8. During firing, sputtering of the vacuum vessel walls occurs. In order to protect sensitive equipment such a cryo-pumps heads, graphite baffles are placed in front of the thruster. The sputtered graphite particles coat the inside of the chamber and the thruster itself with a thin black layer. In an unshielded thruster, this layer is eroded away in the high erosion area near the exit plane. This produces a characteristic white erosion band. In the case of the ISCT200-MS the ceramics walls appear uniformly black, which means that the erosion rate has been reduced to below the deposition rate. Data from other experiments points toward a reduction of a couple orders of magnitude in terms of erosion rates[20, 21].

Additionally, in kilowatt class MS-HT a clear separation appears between the plasma and walls[22, 4]. This effect was not as obvious when operating the ISCT200-MS but a small gap in the plasma allowed us a view all the way to the anode area. This gap was more pronounced near the inner pole[23].

Figure 8. Ceramic walls of the ISCT200-US (left) and ISCT200-MS (right) highlighting, for the MS case, the absence of the characteristic erosion patern in the black deposit formed on the walls.

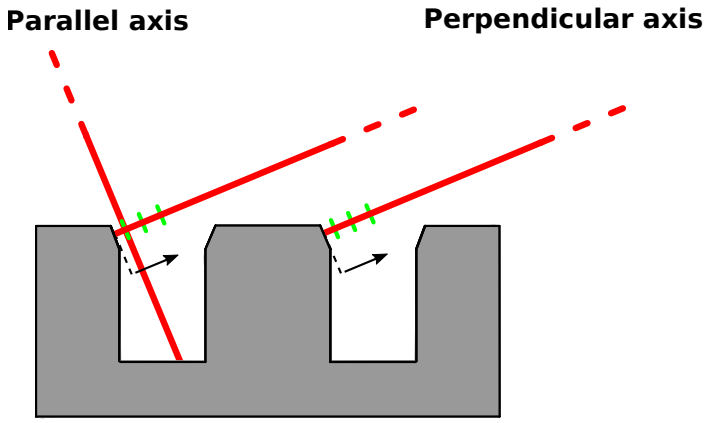

Figure 9. Laser orientation during measurements near the walls of the discharge channel. The arrows are oriented along the positive velocity direction.

4.2. Ion velocity distributions

To measure the ion behavior near the inner and outer wall we took advantage of the beveled edge at the exit of the discharge channel. This bevel is present on both thruster and was initially designed for the ISCT200-US without consideration for the MS configuration. As it can be seen in figure 9 this bevel allows direct measurement of the IVDF normal to the walls. This area shows clear marks of erosion in the unshielded thruster but none in the shielded one (see figure 8).

The IVDF along the axis perpendicular to both the inner (figure 10) and outer (figure 11) walls are measured. For better visibility each plot has been normalized by the maximum value of the IVDFs for each measurement case. The relative amplitude of the IVDFs can not be compared between shielded and unshielded with those plots. The IVDFs show a clear difference in the bulk ion velocity. The majority of the ions

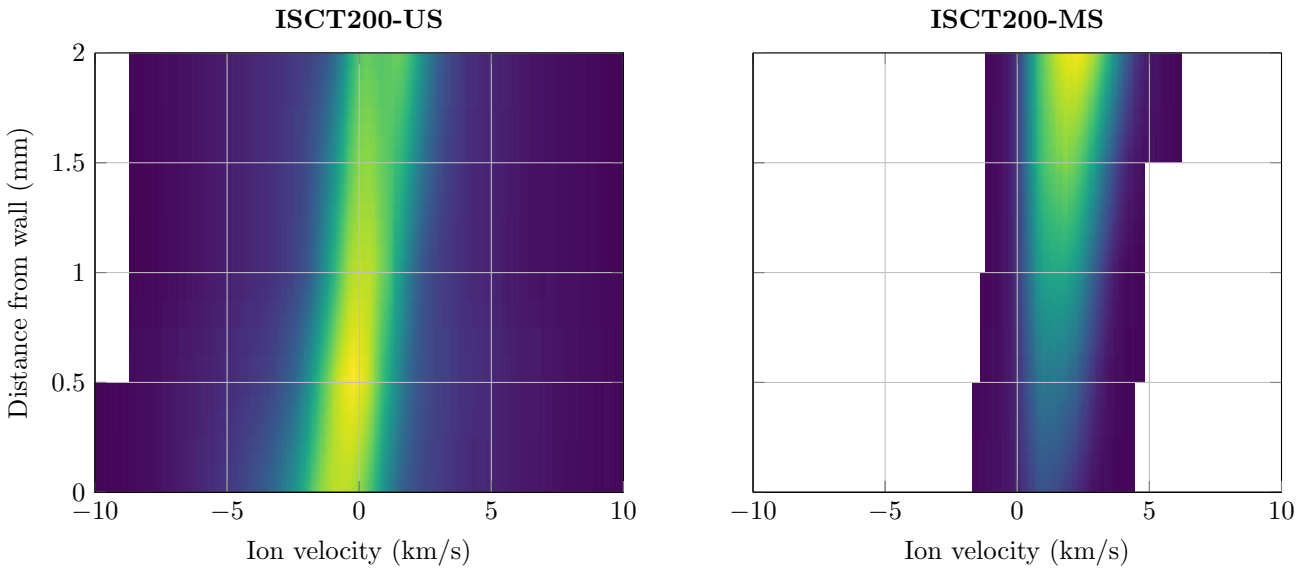

Figure 10. IVDF perpendicular to the internal wall

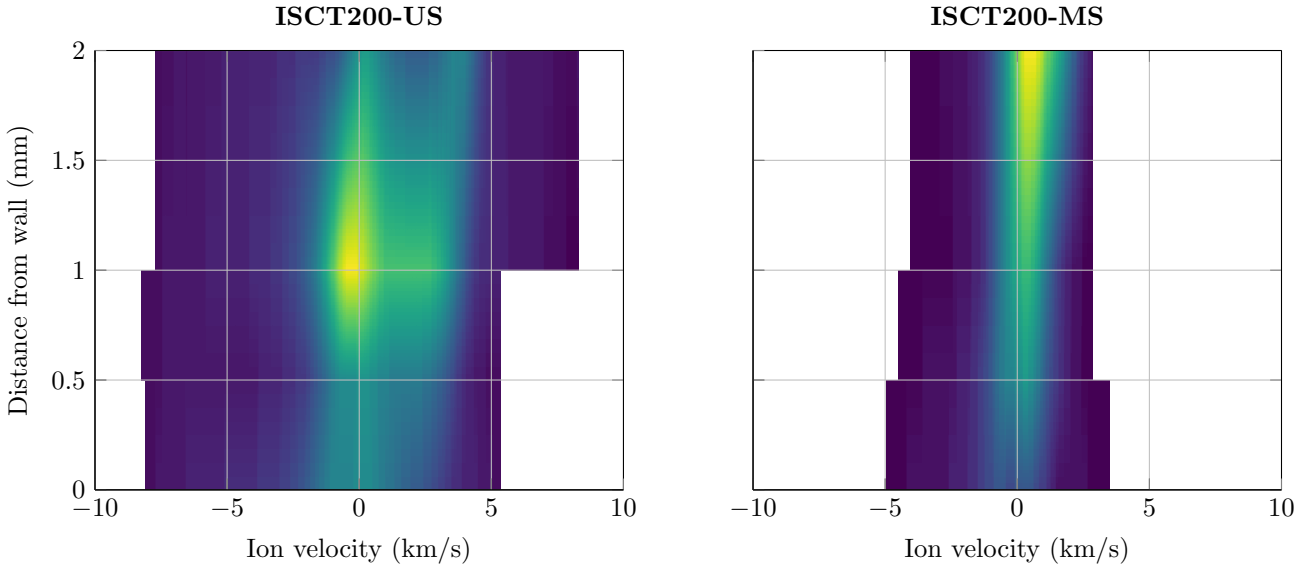

Figure 11. IVDF perpendicular to the external wall

in the US-HT have negative velocity near the walls (i.e. go toward the walls), while they have mostly positive velocities in the MS-HT. The LIF intensity signal, which can be assumed to be proportional to the ion density, is also seen to be sharply decreasing as we approach the wall of the ISCT200-MS while it remains fairly constant in the ISCT200-US. Finally the IVDFs in the unshielded thruster are a lot wider than in the shielded one.

The distribution functions for the ISCT200-MS are roughly Gaussians, pointing toward a single population of ions originating from the same place in the thruster. Some of the IVDF in the unshielded thruster, particularly on the external wall and further

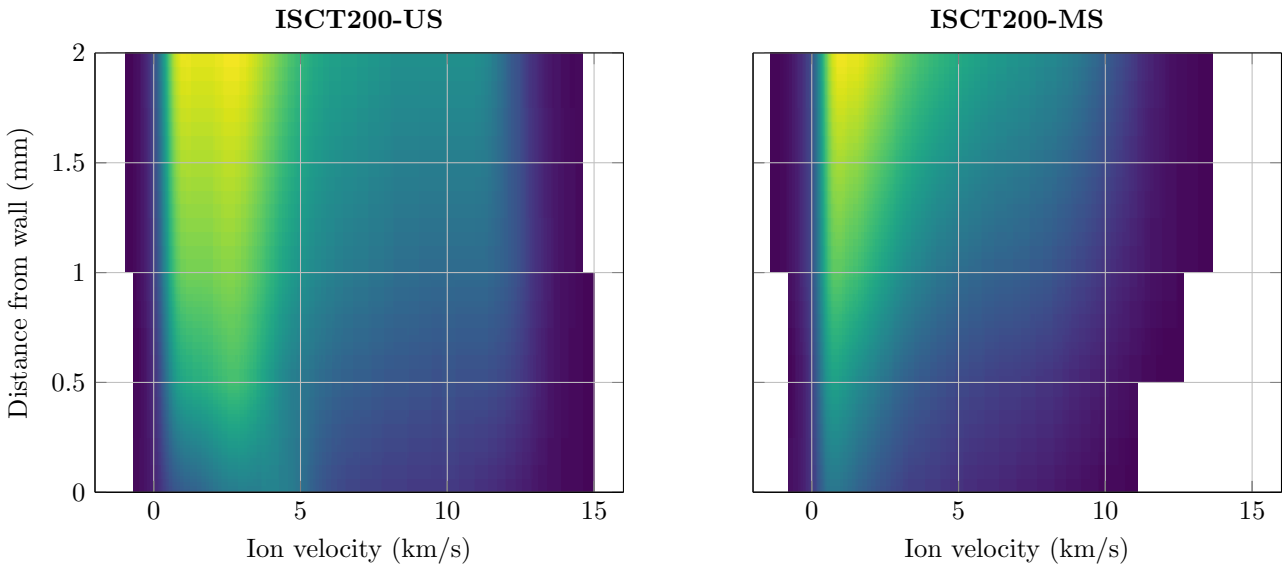

Figure 12. IVDF parallel to the external wall

from the walls, show a double peak structure. Such structure can appear when plasma density is so high that the laser is attenuated. Tests consisting in changing the plasma density (by varying the xenon mass flow) and laser intensity rule out the possibility of total laser absorption attenuating the most intense part of the IVDF.

This means that two populations of ions are observed there. The fainter, higher velocity group is difficult to explain. A possibility is that they are actually fast ions accelerated by the main axial electric field, with their IVDF projected on the slightly oblique laser axis. To be normal to the bevel the laser axis is at a 27 degree angle relative to the radial direction. At the center of the discharge channel ions reach an axial velocity of 10 km/s. On our oblique measurement axis this would translate to a observed velocity of about 4.5 km/s which is very close to what is measured at 2 mm from the bevel. The slower population must thus be created locally. Similar IVDFs have been observed near the walls of the H6 thruster [17].

In order to gather more information about the real two dimensional shape of the IVDFs, the same points as in figure 11 were investigated with the laser parallel to the surface. This method only provides us a second projection of the real two dimensional (ie 2V) velocity distribution. A complete picture of the 2D structure would require optical tomography [24]. Results for the velocity parallel to the external wall bevel are presented in figure 12. Geometric constraints made the same measurements on the internal wall impossible with our setup. Once again two ions groups are apparent in the ISCT200-US. A trail of high velocity ions is visible for both thrusters.

4.3. Ion flux at the walls

From the parallel and perpendicular measurement it is possible to compute both the normal incident velocity and relative ion density. However the two projection axis are

Table 1. Ion density and flux at the walls

Case	n_i (a.u.)	η_{v-}	$\eta_{<-30eV}$
ISCT200-US (inner wall)	723	0.63	0.022
ISCT200-MS (inner wall)	38	0.11	0
ISCT200-US (outer wall)	77	0.54	0.015
ISCT200-MS (outer wall)	19	0.62	0

not enough to extract the incidence angle of the different populations of ions.

The density is computed by assuming that the ratio of the probed metastable ions to ground state ions is constant and the same for both thrusters. Integrating the density functions then give a relative idea of the number of ions present in the probed volume. Great care was taken to ensure that the optical system remains the same when the thrusters are switched. However both collection and laser branch were moved between acquisitions on the internal and external wall. As a result the relative density values can not be compared between those two positions.

Table 1 shows a direct comparison between the results obtained for both thrusters with the IVDF at the wall surface and perpendicular to it.

The relative ion density at the wall (n_i) is a lot lower in the MS-HT than in the US-HT (5% for the inner wall, 25% for the outer wall). This matches visual observations as the plasma in shielded thrusters appears separated from the walls. More particularly in the ISCT200-MS the separation is more obvious for the inner wall than for the outer one.

In table 1 we also define two other important numbers. The first is η_{v-}, the proportion of ion observed going toward the wall. Those ions are the one that should impact the wall and can contribute to the erosion. The second figure is $n_{<-30eV}$, the fraction of ion with an energy superior to 30 eV (around 6.6 km/s for Xe^+) going toward the walls. The 30 eV threshold is chosen because it is the minimum energy ions need to have any significant erosion effect. It is worth noting that this number doesn't capture all the ions with a total energy higher than 30 eV. For example an ion with an incidence angle of 70 degrees and a kinetic energy of 40 eV would only appear on figure 10 and 11 to have a velocity perpendicular to the walls corresponding to 13.7 eV. Considering the long tails of high velocity ions seen on figure 12, such population of ion must be non-negligible.

Nonetheless, there is only 11% of the ions near inner wall of the MS-HT that have negative velocity (i.e. are going toward the wall). In all other cases the proportion is closer to 60%. There was no ion detected with an energy greater than 30 eV for the magnetic shielding case. However we detected a clear fluorescence signal of a small portion of ion with high incoming velocity is the US-HT.

In summary there is both less ions near the walls, and fewer ones with high incoming energy, in the magnetically shielded thruster compared to an equivalent unshielded one.

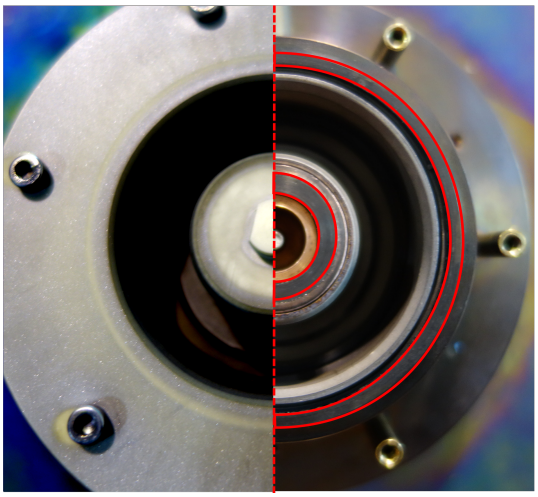

Figure 13. Evidence of erosion above the ceramic caps (left). On the right is a front view of the ISCT200-MS without the caps. The top of the magnetic circuit is highlighted in red [23].

5. Ion behavior near the poles

5.1. Visual evidences of pole erosion

Magnetic pole erosion has been identified as one of the possible failure point in MS-HT. While no erosion is visible in the discharge channel of the H6-MS some marking was observed after on top of the magnetic poles after 150 hours of firing [25, 26]. The eroded areas correspond to the top of the magnetic coils where the magnetic field lines are terminated. Measurements of the erosion rate on the poles have shown that some erosion is present (in the order of 0.1µm/hr) but this erosion rate is two orders of magnitude smaller than the one seen on the walls of US-HT.

In order to observe this pole erosion, alumina "caps" were fitted over the top of the magnetic poles of the ISCT200-MS. Those caps are 1 mm thick. Figure 13 shows the erosion bands seen on the caps after 20 hours of firing. Those erosion bands correspond to the top of the magnetic circuit and are about the same width.

It is worth noting that erosion on the magnetic poles specially on the internal one, is regularly observed in US-HT too. In most Hall thruster the metal parts covering the internal pole exhibits a characteristic surface finish associated with sputtered metal. However, poles erosion is not a failure mode encountered in US-HT as wall erosion is dominating.

5.2. Ion and neutral velocity distribution near the poles

To investigate this erosion zones we performed IVDF measurements at the radius corresponding to the center of the internal and external erosion bands. The plasma density in these area is low. This translates to a lower signal to noise ratio that can make data interpretation complicated [15]. With our small thruster and a 51 mm diameter

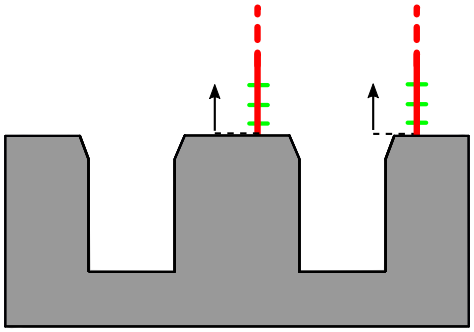

Figure 14. Laser orientation during measurements near the poles of the thrusters. The arrows are oriented along the positive velocity direction

collection lens we were able to get close to the point of interest and collect fluorescence light over a large solid angle. Figure 15 shows the signal quality obtained at the most noisy positions on both the external and internal walls. While excellent signal to noise ratio is achieve all the way to the surface of the internal pole, it was impossible to find any significant signal less than a millimeter away from the external pole. Due to the poor signal to noise ratio near the outer pole, only the results of the inner pole will be presented here.

Figure 16 shows the IVDFs above the inner magnetic pole of the US and MS thrusters. At first glance the IVDFs are shaped similarly. A main ion group is observed coming toward the walls with a normal velocity around 4 to 5 km/s. Another lower density group with the opposite velocity is also seen. Those two groups seem to slow down the further they are from the surface. This might explain the single thermalized group observed at JPL by Jorns [15]. A faint fast group of ions coming toward the wall is also seen in the unshielded ISCT200-US.

The existence of a group of ions with velocities away from the pole surface this close to it made us suspicious of spurious effects caused by measuring close to the surface. We checked if the symmetry in the IVDF was due to a ghost image caused by reflection of the laser on the pole surface. Figure 17 presents the IVDF 2 mm above the internal pole of the shielded thruster with a laser normal to the surface and one canted 20 degrees. With this angle the specular reflection of the laser does not intercept the measurement volume. we found that the positive velocity group is still present and has the same amplitude.

Another possibility we considered is that this population is actually ions that have had an elastic collision with the pole. However most ions colliding with the wall should be neutralized. The fast ions would then need to have been produced from these neutrals on a distance less than a couple of millimeters. To investigate this possibility we looked for fast neutrals resulting from ions bouncing on the surface and being neutralized. Figure 18 shows the neutral velocity density function (NVDF) 1 mm above the inner pole of the MS-HT. There is no evidence of any group of neutrals in the +3 to +4 km/s range.

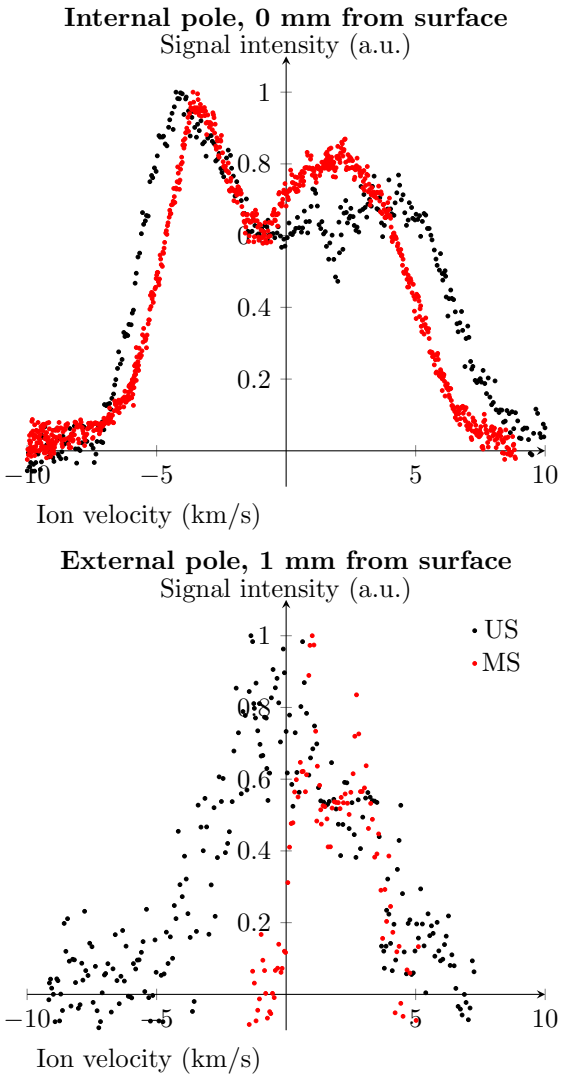

Figure 15. Worst signal to noise raio normalized IVDFs above the internal and external magnetic poles

Neither laser reflection nor ion elastic collisions can explain this symmetric double peak structure. The magnetic field isn't strong enough to have any magnetic mirroring effect on the ions. One possible explanation could come from an inverted sheath caused by strong secondary electron emission. Such inverted sheath has been observed in simulation in the high electron temperature areas inside Hall thrusters [27]. This inverted sheath could reflect some ions back downstream. However those inverted sheath are associated with high electron temperatures (> 30 eV), which are present above the poles in MS-HT but not in US-HT. This structure was present both on the stainless steel pole piece and the alumina one.

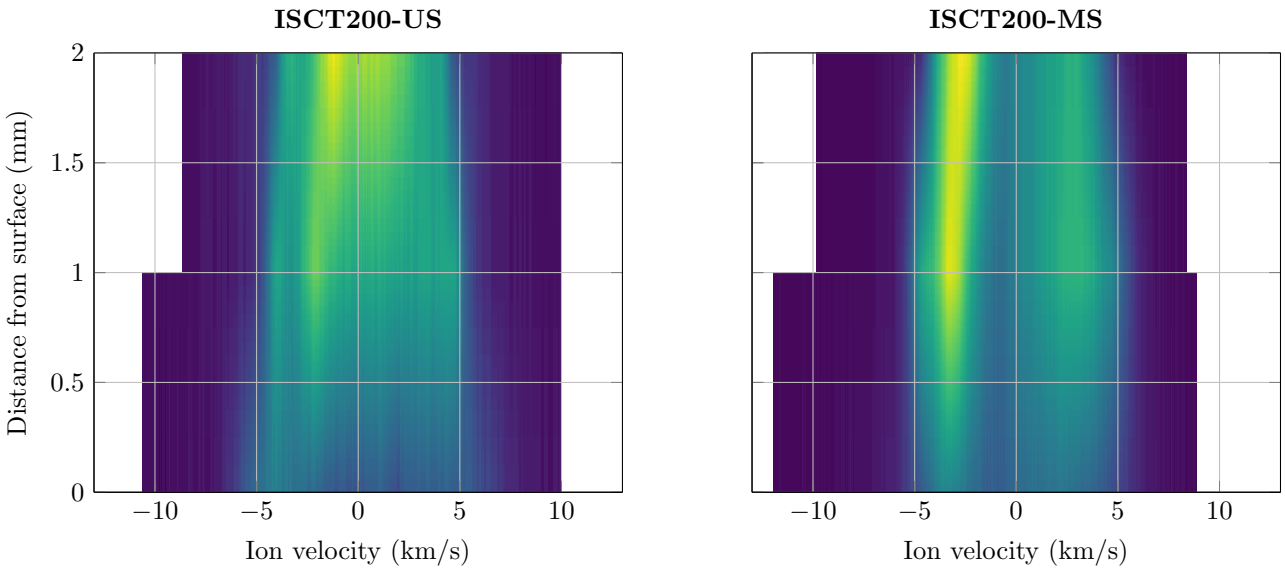

Figure 16. IVDF perpendicular to the inner magnetic pole

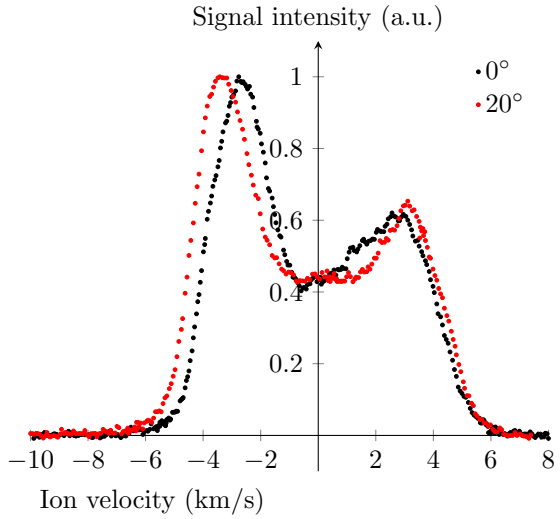

Figure 17. IVDF 2 mm above the internal pole of the ISCT200-MS with the laser firing along the thruster axis (0°) and off-axis (20°)

6. Conclusion

Our results show multiple effects of the magnetic shielding configuration on the ion behavior that helps understand the reduction in erosion observed.

The non-intrusive LIF spectroscopy measurements have confirmed that in a magnetically shielded Hall thruster the electric field is located outside the discharge channel. As a consequence the plasma potential inside the channel is nearly constant and most of the ionization happens outside the thruster itself. This contributes to both a lower ion density and lower ion energy inside the thruster.

A small population of ions with a high velocity normal to the walls is observed in

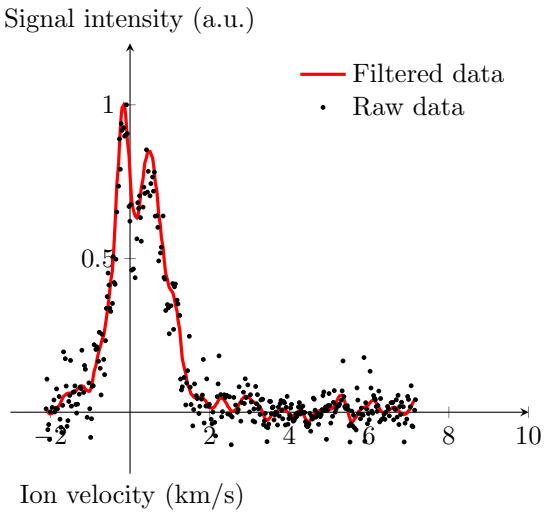

Figure 18. NVDF 1 mm above the internal pole of the ISCT200-MS

the unshielded thruster. This population could be responsible to important part of the erosion channel walls. In the shielded thruster this population isn't detected. The bulk ion velocity is also pointing away from the walls. Furthermore the ion density sharply decrease has it gets closer to the walls.

Finally measurements above the magnetic poles yield IVDF normal to the surface with a symmetric "double peak" structure for both US and MS thrusters. This peculiar structure does not seems to be explainable by laser reflection nor elastic collision effects with the thruster surface. Both thrusters have similarly shaped IVDF in this area. There is no evidence of any phenomenon that would increase pole erosion in a magnetically shielded thruster compared to a standard one.

7. Ackowledgements

We are indebted to Julien Vaudolon who developed and tested the first version of the ISCT200-MS, for his insightful advices and many discussions we had on the concept of magnetic shielding.

This work was done as part of the a CNES research program. It has been financially supported by the CNES and the Région Centre council.

[1] Frederic Marchandise, Nicolas Cornu, Frank Darnon, and Denis E. PPS®1350-G Qualification status 10500 h. *30th International Electric Propulsion Conference*, pages IEPC–2007–164, 2007.

[2] Ryan Conversano. *Low-Power Magnetically Shielded Hall Thrusters*. PhD thesis, Univeristy of California, Los Angeles, 2015.

[3] Ioannis Mikellides, Ira Katz, Richard Hofer, Dan Goebel, Kristi de Grys, and Alex Mathers. Magnetic Shielding of the Acceleration Channel Walls in a Long-Life Hall Thruster. In *46th AIAA/ASME/SAE/ASEE Joint Propulsion Conference & Exhibit*, number July, pages AIAA 2010–6942, Nashville, TN, jul 2010. American Institute of Aeronautics and Astronautics.

[4] Ioannis G. Mikellides, Ira Katz, Richard R. Hofer, Dan M. Goebel, Kristi de Grys, and Alex

Mathers. Magnetic shielding of the channel walls in a Hall plasma accelerator. *Physics of Plasmas*, 18(3):033501, 2011.

[5] Ioannis Mikellides, Ira Katz, and Richard Hofer. Design of a Laboratory Hall Thruster with Magnetically Shielded Channel Walls, Phase I: Numerical Simulations. In *47th AIAA/ASME/SAE/ASEE Joint Propulsion Conference & Exhibit*, number August, pages 1–18, San Diego, California, jul 2011. American Institute of Aeronautics and Astronautics.

[6] Ioannis G Mikellides, Ira Katz, Hani Kamhawi, Jonathan L Vannoord, and National Aeronautics. Numerical Simulations of a 20-kW Class Hall Thruster Using the Magnetic-Field-Aligned-Mesh Code Hall2De. *IEPC*, pages 1–12, 2011.

[7] Ioannis G Mikellides, Richard R. Hofer, Ira Katz, and Dan M. Goebel. The Effectiveness of Magnetic Shielding in High-Isp Hall Thrusters. In *49th AIAA/ASME/SAE/ASEE Joint Propulsion Conference*, pages 1–18, San Jose, CA, jul 2013. American Institute of Aeronautics and Astronautics.

[8] Benjamin Jorns, Dan M. Goebel, and Richard R. Hofer. Plasma Perturbations in High-Speed Probing of Hall Thruster Discharge Chambers: Quantification and Mitigation. In *51st AIAA/SAE/ASEE Joint Propulsion Conference*, Reston, Virginia, jul 2015. American Institute of Aeronautics and Astronautics.

[9] Lou Grimaud, Aude Pétin, Julien Vaudolon, and Stéphane Mazouffre. Perturbations induced by electrostatic probe in the discharge of Hall thrusters. *Review of Scientific Instruments*, 87(4):043506, apr 2016.

[10] Lou Grimaud, Julien Vaudolon, and Stéphane Mazouffre. Design and characterization of a 200 W low power Hall thruster in "magnetic shielding" configuration. In *Space Propulsion Conference*, number May, Rome, 2016.

[11] S Mazouffre, P Echegut, and M Dudeck. A calibrated infrared imaging study on the steady state thermal behaviour of Hall effect thrusters. *Plasma Sources Science and Technology*, 16(1):13–22, feb 2007.

[12] Dan M. Goebel, Richard R. Hofer, Ioannis G. Mikellides, Ira Katz, James E. Polk, and Brandon N. Dotson. Conducting Wall Hall Thrusters. *IEEE Transactions on Plasma Science*, 43(1):118–126, jan 2015.

[13] Stéphane Mazouffre. Laser-induced fluorescence diagnostics of the cross-field discharge of Hall thrusters. *Plasma Sources Science and Technology*, 22(1):013001, feb 2013.

[14] Stéphane Mazouffre. Laser-induced fluorescence spectroscopy applied to electric thrusters. In *Electric Propulsion Systems: from recent research developments to industrial space applications - STO-AVT-263*, pages 10–1. Von Karman Institute for fluid dynamics, vki lectur edition, 2016.

[15] Benjamin Jorns, Christopher A. Dodson, John R. Anderson, Dan M. Goebel, Richard R. Hofer, Michael J. Sekerak, Alejandro Lopez Ortega, and Ioannis G. Mikellides. Mechanisms for Pole Piece Erosion in a 6-kW Magnetically-Shielded Hall Thruster. In *52nd AIAA/SAE/ASEE Joint Propulsion Conference*, number July, pages 1–21, Salt Lake City, UT, jul 2016. American Institute of Aeronautics and Astronautics.

[16] Julien Vaudolon and Stéphane Mazouffre. Indirect determination of the electric field in plasma discharges using laser-induced fluorescence spectroscopy. *Physics of Plasmas*, 21(9):093505, sep 2014.

[17] Wensheng Huang, Alec D. Gallimore, and Timothy B. Smith. Interior and Near-Wall Ion Velocity Distribution Functions in the H6 Hall Thruster. *Journal of Propulsion and Power*, 29(5):1146–1154, sep 2013.

[18] S Mazouffre, V Kulaev, and J Pérez Luna. Ion diagnostics of a discharge in crossed electric and magnetic fields for electric propulsion. *Plasma Sources Science and Technology*, 18(3):034022, aug 2009.

[19] A Lejeune, G Bourgeois, and S Mazouffre. Kr II and Xe II axial velocity distribution functions in a cross-field ion source. *Phys. Plasmas Phys. Plasmas Additional information on Phys. Plasmas Journal Homepage*, 19(19):73501–63507, 2012.

[20] Richard R Hofer, Dan M Goebel, Ioannis G Mikellides, and Ira Katz. Magnetic shielding of a laboratory Hall thruster. II. Experiments. *Journal of Applied Physics*, 115(4):043304, jan 2014.

[21] Ioannis G. Mikellides, Ira Katz, Richard R. Hofer, and Dan M. Goebel. Magnetic shielding of walls from the unmagnetized ion beam in a Hall thruster. *Applied Physics Letters*, 102(2):13–18, 2013.

[22] Stephane Mazouffre, Julien Vaudolon, Guillaume Largeau, Carole Henaux, Alberto Rossi, and Dominique Harribey. Visual Evidence of Magnetic Shielding With the PPS-Flex Hall Thruster. *IEEE Transactions on Plasma Science*, 42(10):2668–2669, oct 2014.

[23] Lou Grimaud, Julien Vaudolon, Stephane Mazouffre, and Claude Boniface. Design and characterization of a 200W Hall thruster in "magnetic shielding" configuration. In *52nd AIAA/SAE/ASEE Joint Propulsion Conference*, pages 1–17, Salt Lake City, UT, jul 2016. American Institute of Aeronautics and Astronautics.

[24] R. Koslover and R. McWilliams. Measurement of multidimensional ion velocity distributions by optical tomography. *Review of Scientific Instruments*, 57(10):2441, 1986.

[25] Ioannis G Mikellides and Alejandro Lopez Ortega. Assessment of Pole Erosion in a Magnetically Shielded Hall Thruster. *50th AIAA/ASME/SAE/ASEE Joint Propulsion Conference*, 2014.

[26] Michael J Sekerak, Richard R Hofer, James E Polk, Benjamin a Jorns, and Ioannis G Mikellides. Wear Testing of a Magnetically Shielded Hall Thruster at 2000 s Specific Impulse. In *34th International Electric Propulsion Conference*, pages 1–37, 2015.

[27] Francesco Taccogna. Non-classical plasma sheaths: space-charge-limited and inverse regimes under strong emission from surfaces. *The European Physical Journal D*, 68(7):199, jul 2014.